LWT - Food Science and Technology 149 (2021) 111999

Contents lists available at ScienceDirect

LWT

journal homepage: www.elsevier.com/locate/lwt

Effect of heat-treated tea water-insoluble protein nanoparticles on the characteristics of Pickering emulsions

Zhongyang Ren [a,b,c], Zhongzheng Chen [b], Yuanyuan Zhang [b], Xiaorong Lin [b], Zhanming Li [c,e], Wuyin Weng [a], Hongshun Yang [c,d,**], Bin Li [b,*]

[a] College of Food and Biological Engineering, Jimei University, Xiamen, 361021, China
[b] College of Food Science, South China Agricultural University, 483 Wushan Street, Tianhe District, Guangzhou, 510642, China
[c] Department of Food Science & Technology, National University of Singapore, Science Drive 2, Singapore, 117542, Singapore
[d] National University of Singapore (Suzhou) Research Institute, 377 Lin Quan Street, Suzhou Industrial Park, Suzhou, Jiangsu, 215123, PR China
[e] School of Grain Science and Technology, Jiangsu University of Science and Technology, Zhenjiang, 212004, China

ARTICLE INFO

Keywords:
Tea residue
Protein nanoparticle
Pickering emulsion
Heat treatment
Gel

ABSTRACT

Tea water-insoluble protein nanoparticles (TWIPNs) can be used as Pickering particles. However, Pickering emulsions stabilized by heat-treated TWIPNs (TWIPNPEs) were not characterized clearly. Therefore, the effect of heat-treated TWIPNs on the characteristics of Pickering emulsions was analyzed. TWIPNs became small at 60 °C and reassembled at 100 and 120 °C. Disulfide bonds and noncovalent bonds synergistically participated in the intermolecular forces of heat-treated TWIPNs. The random coil content of heat-treated TWIPNs decreased from 0.24 to 0.13 and the contents of α-helices and β-sheets increased from 0.11 to 0.27 to 0.19 and 0.30 in the proportion of secondary structure with the increase in heat-treated TWIPN temperature. High temperature (100 °C/120 °C) on TWIPN accelerated the flocculation of emulsion droplets. A potential mechanism for the changes occurring in TWIPNPEs based on heat-treated TWIPNs was proposed to exhibit the instability of TWIPNPEs stabilized by heat-treated TWIPNs due to the structural rearrangements and enhanced intermolecular forces of TWIPNs at 100 and 120 °C. Besides, heat-treated TWIPNs at 30 and 40 g/L decreased the gel-like behavior of TWIPNPEs. These results can broaden our understanding of the characteristics of TWIPNPEs stabilized by heat-treated TWIPNs for utilizing tea by-products.

1. Introduction

Some solid particles have a unique ability of partial wettability in both water and oil phases to form stable emulsions, which is commonly defined as Pickering emulsions (Chevalier & Bolzinger, 2013). Compared with emulsions stabilized by conventional emulsifiers such as low-molecular-weight surfactants, emulsions stabilized by Pickering particles, especially food-grade protein particles, possess many potential advantages such as the reduction in the lipid oxidation and delivery of a functional substance (Nikbakht Nasrabadi, Sedaghat Doost, Goli & Van der Meeren, 2020; Zhou, Yan, Yin, Tang, & Yang, 2018). Chemical and physical treatments are commonly applied to deal with proteins for better-utilizing proteins to stabilize Pickering emulsions.

Heat treatment, as a kind of physical treatments, has been extensively applied to alter the physicochemical characteristics and structure of water-soluble proteins (Wu et al., 2015). Heat treatment can also accelerate protein degradation (Chen et al., 2021). Studies have investigated the effect of heat treatment of proteins on the characteristics of protein-based emulsions. Proteins are only suitable as Pickering particles if they form particles. Some water-soluble proteins in their native form are not suitable as Pickering particles, such as milk proteins (Ho et al., 2018), mushroom polyphenol oxidases (Baltacıoğlu, Bayındırlı, Severcan, & Severcan, 2015), soy proteins (Keerati, 2009; Wang et al., 2019), peanut proteins (Shen et al., 2015), winged bean proteins (Makeri, Muhammad, Ghazali, & Mohammed, 2019) and so on. Some water-soluble proteins after heat treatment could be utilized to stabilize Pickering emulsions such as soy proteins (Liu & Tang, 2013), peanut proteins (Ning et al., 2020).

Whey protein solution processed at the temperatures of 60–90 °C exhibits a decline trend in emulsifying ability (Millqvist-Fureby,

** Corresponding author.
* Corresponding author. Department of Food Science & Technology, National University of Singapore, Science Drive 2, Singapore, 117542, Singapore.
E-mail addresses: fstynghs@nus.edu.sg (H. Yang), bli@scau.edu.cn (B. Li).

https://doi.org/10.1016/j.lwt.2021.111999
Received 3 February 2021; Received in revised form 22 June 2021; Accepted 23 June 2021
Available online 29 June 2021

Elofsson, & Bergenståhl, 2001). The formation of large protein aggregates is due to heat treatment and protein aggregates cover the emulsion droplets inefficiently, resulting in emulsion instability (Raikos, 2010). Besides, the loss of absorption behavior of proteins at the heat treatments is not beneficial for the formation of the interface layer in contrast to the untreated proteins. Thus, the heat treatment of water-soluble proteins results in the reduction of emulsifying efficiency under certain conditions, which is related to the degree of protein denaturation (Ananey-Obiri et al., 2018). All these reports indicate that protein emulsifiers are influenced by heat treatment. Protein-based Pickering particles are different from these protein emulsifiers.

Pickering emulsions can be stabilized by plant water-insoluble protein particles, which are Pickering particles such as pea proteins (Liang & Tang, 2014), zeins (Zou, Guo, Yin, Wang, & Yang, 2015), kafirins (Xiao, Wang, Gonzalez, & Huang, 2016), gliadins (Chen, McClements, et al., 2018; Liu, Liu, Guo, Yin, & Yang, 2017) and tea water-insoluble protein nanoparticles (TWIPNs) (Ren, Chen, Zhang, Lin, & Li, 2019). Some studies have focused on the effect of heat treatment on the properties of water-insoluble proteins such as zeins (Sun et al., 2016) and kafirins (Emmambux & Taylor, 2009). TWIPNs, as the most component in the tea wastes, are obtained by alkali-solution and acid-precipitation method from tea wastes (Ren, Chen, Zhang, Lin, & Li, 2019). TWIPNs can form gel-like PE after high-pressure homogenization (Ren, Chen, Zhang, Lin, & Li, 2020). As previously reported, TWIPN-stabilized Pickering emulsions (TWIPNPEs) can be used as the template of oil gel preparation (Ren et al., 2021). However, how heat treatment affects the emulsification of TWIPNs is still unclear, especially in the characteristics of TWIPNPE prepared using heat-treated TWIPNs.

Therefore, the present study aimed to determine the effect of heat-treated TWIPNs on the characteristics of TWIPNPEs for the potential application of TWIPNPEs in different environments. The properties of TWIPNs heated at different temperatures (60, 100 and 120 °C) were determined. Furthermore, the effect of heat treatment of TWIPNs on the characteristics and rheological behavior of TWIPNPEs was analyzed.

2. Materials and methods

2.1. Materials

TWIPNs were prepared in the bioengineering laboratory of South China Agricultural University (Guangzhou, China) (Ren, Chen, Zhang, Lin, & Li, 2019). Briefly, tea residues were extracted at 90 °C for 1.5 h using 0.3 mol/L NaOH solution according to a ratio of tea residues and solution (1:30, g/mL). The mixtures were centrifuged at 8288 *g* for 15 min. Then the supernatant was decolored with 333 g/L H_2O_2 for 24 h and precipitated at pH 3.5. The precipitates were washed to the neutral and frozen-drying via a freeze drier (Christ, ALPHA 1–2 LD Plus, Osterode, Germany) to gain TWIPNs. Soy oil was purchased from the LOTUS supermarket in China. NaOH and KBr were of analytical purity. Silicon wafers were used for atomic force microscopy (AFM) (AFM workshop, Signal Hill, California, USA). All water was of deionized water.

2.2. Heat treatment of TWIPNs

Heat treatment of TWIPNs was implemented according to a previously published method with some modifications (Sarkar et al., 2016). According to the temperatures of pasteurization, sterilization/cooking and autoclaving, three temperatures (60, 100 and 120 °C) were chosen for this experiment. The TWIPN suspension was heated in a water bath at 60 and 100 °C for 30 min, respectively. The TWIPN suspension of 100 mL was processed using an oil bath at 120 °C for 30 min. After cooling to 25 ± 3 °C, the TWIPN suspension was dried using frozen-drying. The TWIPN suspension at the concentration of 5–40 g/L was prepared with deionized water and stirred for 2 h and hydrated for 24 h at 4 °C. The suspension was adjusted to pH 7.0 using 1.0 mol/L NaOH solution. The TWIPN suspension was used for tests and preparing emulsions immediately.

2.3. Measurement of TWIPN characteristics

2.3.1. Particle size and zeta potential

Liquid samples of different TWIPN concentrations at pH 7.0 were diluted 100 times using deionized water before testing. The test condition was equilibration for 60 s and the automatic run number of 10 times at 25 °C. The cell type was glass cuvettes. The hydrodynamic diameter (D_H) and zeta potential of the samples were tested via particle size and zeta potential analyzer (NanoBrook, 90 Plus Zeta, NewYork, USA) according to a previous method (Xue, Wang, Hu, Zhou, & Luo, 2018).

2.3.2. Pattern of intra-particle interactive forces

The intra-particle interactive forces of TWIPN structure at different temperatures were determined according to a previous method (Liu & Tang, 2016). The TWIPN dispersions (20 g/L) in different solvents like deionized water, 6 mol/L urea, 10 g/L SDS, 30 mmol/L dithiothreitols (DTT) alone or in combination was prepared. The mixtures were stirred for 30 min. The mixtures were diluted 100 times using the deionized water before testing. The D_H of samples was analyzed.

2.3.3. Ultraviolet spectroscopy

The ultraviolet absorption spectra of TWIPNs suspension after diluting to an appropriate dilution using deionized water were determined using a spectrophotometer (SHIMAZU, UV-1800, Kyoto, Japan). The scanning range was 200–450 nm at a medium speed of 200 nm/min.

2.3.4. Fourier transform infrared spectroscopy

Samples were analyzed using a Fourier transform infrared spectrometer (FTIR) (Vertex 70, Hamburg, Germany) referred to a previously reported method with some modifications (Sow, Tan, & Yang, 2019). TWIPN samples (1.0 mg) were mixed with KBr (99.0 mg) and pressed into a tablet. The test condition was 64 scan times at 4000-500 cm^{-1} and a resolution of 4 cm^{-1}. Origin software (Origin Lab, Pro 9.0.5, Northampton, Massachusetts, USA) was used to analyze the spectra of amide I (1700-1600 cm^{-1}) and quantify the secondary structures of TWIPNs.

2.3.5. Atomic force microscopy

TWIPNs were analyzed via AFM (AFM workshop, Signal Hill, California, USA) as a previous report (Chen, Zhou, et al., 2018). The TWIPN solution was dropped on a cleaved silicon wafer surface and dried. The number of scan lines was 512. The scan rate was 0.4 Hz. Gwyddion 2.53 software from Petr Klapetek was used to analyze the results.

2.4. Preparation of TWIPNPEs

TWIPNPEs were prepared at the different concentrations of heat-treated TWIPNs according to a previous method (Ren et al., 2021). The pH of the suspension with different TWIPN concentrations (5–40 g/L) was adjusted to 7.0 using 1.0 mol/L NaOH. At a fixed oil-water ratio of 6:4 (mL:mL), the suspension (40 mL) at TWIPN concentrations was mixed with soy oils (60 mL) using a shear emulsifying machine (SUOTN, 50 CE0S–H, Shanghai, China) at 20,000 r/min for 2 min and further homogenized once at 40 MPa via a high-pressure homogenizer (AH-Basic-II, Suzhou, China).

2.5. Measurements of droplet size and flocculation index of TWIPNPEs

The emulsion droplet size and particle size distribution were measured using a Mastersizer (Malvern 3000, Malvern, UK) according to a reported method (Liu & Tang, 2016). Deionized water and 10 g/L

sodium dodecyl sulfate (SDS) solution were used as dispersants. Every test was performed from washing, removing background and adding samples to testing. The volume-average droplet size ($d_{4,3}$) of TWIPNPEs was determined. The flocculation index (FI) of TWIPNPEs were calculated using Eq. (1).

$$FI\ (\%) = (d_{4,3-W} / d_{4,3-S} - 1) \times 100 \quad (1)$$

where $d_{4,3\text{-}W}$ and $d_{4,3\text{-}S}$ are the volume-average droplet sizes of emulsions in deionized water and 10 g/L SDS dispersion, respectively.

2.6. Determination of creaming index of TWIPNPEs

The creaming index (CI) of TWIPNPEs was determined according to a previous method (Liu & Tang, 2013). TWIPNPEs were added to a 10 mL glass tube. The height of the serum in the emulsions (H_s) was measured over 50 days. The CI of TWIPNPEs was calculated according to the percentage of serum height in the height of initial emulsions.

2.7. Morphological observation of TWIPNPEs

The morphology of TWIPNPEs was observed initially via optical microscope (Motic, BA310-T, Hong Kong, China) equipped with a Motic Image Advanced 3.2 system. The TWIPNPEs were diluted five times and the photos were gained using a 100 × lens.

2.8. Determination of rheological properties of TWIPNPEs

The viscoelasticity of TWIPNPEs was measured using a rheometer (Anton Paar, MCR-102, Graz, Austria) according to a previously published method (Tan et al., 2019). The apparent viscosity of TWIPNPEs was tested at shear rates from 0.1 to 100 s^{-1} using a parallel plate (diameter 50 mm). The storage modulus (G′) and loss modulus (G″) at angular velocities of 0.1–100 rad/s were determined within a small amplitude oscillatory frequency sweep mode. The gap was fixed at 1.0 mm during the test. The temperature was 25 ± 0.1 °C for the above measurements.

2.9. Statistical analysis

Each test was performed in triplicate. The data were expressed as the mean values ± standard deviation. Origin Pro 9.0.5 software was applied to evaluate the differences among the test results according to a one-way analysis of variance (ANOVA) test ($P < 0.05$).

3. Results and discussion

3.1. Effect of heat treatment on TWIPN characteristics

3.1.1. D_H, zeta potential and particle size distribution of TWIPNs

The physical, structure and morphological characteristics of protein particles are important for the stability and rheological behavior of Pickering emulsions. Heat treatment extremely affects the physicochemical properties of proteins. Therefore, the effects of the heat treatment on the characteristics of TWIPNs were firstly analyzed. The D_H, polydispersity index (PDI), zeta potential and particle size distribution of the TWIPN suspension at different temperatures (60, 100 and 120 °C) are shown in Table S1 and Fig. 1. The change in the particle size distribution of TWIPNs at different concentrations with the increase in temperature had the same trend. The TWIPN concentration of 20 g/L was chosen for the particle size distribution. Under the same heat treatment, the D_H of TWIPNs increased with increasing TWIPN concentrations; however, the D_H of TWIPNs at the same TWIPN concentration exhibited a decreased trend at 60 °C and then reassembled at 100 and 120 °C, which showed a medium dispersed system with PDIs of 0.43–0.75 (Table S1), indicating that TWIPNs were heterogeneously distributed.

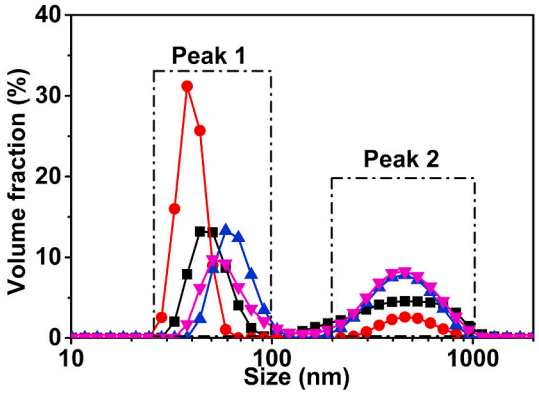

Fig. 1. Volume fraction of tea water-insoluble protein nanoparticle suspension (20 g/L) at different tempertatures. (■, Unheated; ●, 60 °C; ▲, 100 °C; ▼, 120 °C.)

The zeta potential was mainly affected by TWIPN concentration. The zeta potential increased with the increase in the TWIPN concentration. The absolute value of zeta potential was more than 30 mV indicating that the suspension was relatively stable (Table S1), as previously reported (Sow, Chong, Xu, & Yang, 2018). Furthermore, the particle size distribution of heat-treated TWIPNs was bimodal (Fig. 1). The range of particle size distribution was 20–1000 nm and the values of both peaks were approximately 50 nm and 450 nm, respectively. Compared with that of the unheated TWIPNs, the volume fraction of heat-treated TWIPNs increased in peak 1 and decreased in peak 2, which was consistent with the D_H decrease in TWIPNs heat-treated at 60 °C. However, the increase of volume fraction in peak 2 indicated that TWIPNs regathered to form large particles in the suspension at 100 and 120 °C (Fig. 1).

3.1.2. Intra-particle interactive forces of TWIPNs

To clarify the interactions of TWIPN particles on the different heat treatment conditions, the intra-particle interactive forces of heat-treated TWIPNs were determined (Table 1). In most cases, SDS, urea and DTT disrupt hydrophobic interaction, hydrogen bonds and disulfide bonds, respectively (Schmitt et al., 2010). In the presence of SDS and urea alone, the D_H of TWIPNs decreased compared with that of TWIPNs without protein-perturbing solvent treatment (Blank, Table 1). The D_H of TWIPNs under the different heat treatments decreased largely in the existence of both SDS and DTT, which was lower than that in the existence of Urea, SDS and DTT alone. These results indicated that the interaction between the TWIPNs mainly depended on noncovalent bonding forces such as hydrophobic interactions and disulfide bonds. Meanwhile, the synergistic effect was found between the hydrophobic interactions and disulfide bonds according to the D_H of TWIPNs dealt with SDS, DTT and SDS + DTT.

Under the treatment of Urea, DTT, Urea + DTT and Urea + SDS + DTT, the D_H of the TWIPNs had a trend of decreasing at 60 and 100 °C and increasing at 120 °C, indicating that hydrogen bonds and disulfide bonds between the TWIPNs were susceptibly affected by heat treatment. After heat treatment, the noncovalent bonds remained the main force; meanwhile, the disulfide bonds also participated in the interaction forces between the TWIPNs. These results indicated that disulfide bonds and noncovalent bonds synergistically participated in the intermolecular forces of heat-treated TWIPNs. Besides, both hydrophobic interactions and disulfide bonds are important for sustaining the nanoparticle structure to stabilize Pickering emulsions (Liu & Tang, 2016).

3.1.3. Ultraviolet absorption spectrum of TWIPNs

Besides, protein structures can be illustrated using the ultraviolet

Table 1
Effects of the different protein-perturbing solvents on D_H of tea water-insoluble protein nanoparticles at different temperatures.

protein-perturbing solvents	D_H (nm)			
	Unheated	60 °C	100 °C	120 °C
Blank	348.66 ± 19.62^{a}	275.1 ± 22.32^{a}	331.64 ± 28.14^{a}	370.87 ± 11.46^{a}
Urea	170.25 ± 5.24^{c}	197.75 ± 8.24^{b}	135.99 ± 6.20^{e}	285.15 ± 13.80^{bc}
SDS	147.05 ± 5.00^{cd}	175.70 ± 3.68^{c}	168.75 ± 2.62^{cde}	162.62 ± 17.62^{d}
Urea + SDS	172.43 ± 14.01^{c}	205.17 ± 8.98^{b}	191.05 ± 4.61^{de}	188.39 ± 13.33^{d}
DTT	331.15 ± 32.74^{a}	213.06 ± 22.64^{b}	203.06 ± 32.23^{b}	380.00 ± 25.58^{a}
Urea + DTT	219.80 ± 11.32^{b}	220.40 ± 14.84^{b}	199.72 ± 3.92^{bcd}	307.30 ± 22.87^{b}
SDS + DTT	133.99 ± 4.01^{d}	144.85 ± 7.57^{d}	148.58 ± 1.18^{e}	125.06 ± 3.85^{e}
Urea + SDS + DTT	357.55 ± 10.07^{a}	281.87 ± 17.08^{a}	211.94 ± 19.37^{bc}	264.18 ± 0.38^{c}

*SDS and DTT represent sodium dodecyl sulfate and dithiothreitol, respectively. Values are given as means ± SD from triplicate tests. Lowercase indicates differences between the different protein-perturbing solvents at the same temperature ($P < 0.05$).

absorption spectrum. The ultraviolet absorption spectra of TWIPNs heated at different temperatures are shown in Fig. 2. Proteins usually have strong absorption at approximately 280 nm in the ultraviolet absorption region. TWIPNs had a strong absorption peak at 277 nm. The ultraviolet absorption intensity of TWIPNs increased after heat treatment, especially for TWIPNs heated at 120 °C. The ultraviolet absorption spectra of protein change with the increase in the temperature, especially at high temperatures (Wada, Fujita, & Kitabatake, 2006). Similarly, the ultraviolet absorption of the ovotransferrin groups increases after heat treatment (Tong et al., 2012). These results indicated the conformation change of TWIPNs.

3.1.4. FTIR analysis of TWIPNs

Subsequently, the FTIR of TWIPNs was applied to analyze the secondary structures. Amide I and amide II peaks appeared at approximately 1550 cm^{-1} and 1650 cm^{-1}, respectively (Li, Bai, et al., 2020; Ren, Chen, Zhang, Lin, & Li, 2019). The peak of amide I was taller than that of amide II. Therefore, we chose amide I to analyze the secondary structures. The secondary structures of heat-treated TWIPNs at the wavenumbers of 1600–1700 cm^{-1} are shown in Table S2. The β-sheet (1610-1642 cm^{-1}), random coil (1642-1650 cm^{-1}), α-helix (1650-1660 cm^{-1}), β-turn (1660-1680 cm^{-1}) and β-antiparallel (1680-1700 cm^{-1}) were identified (Carbonaro & Nucara, 2010; Ren, Chen, Zhang, Lin, & Li, 2019). With the increase in temperature, the contents of random coil decreased from 0.24 to 0.13 and the contents of α-helices and β-sheets increased from 0.11 to 0.27 to 0.19 and 0.30 in the proportion of secondary structure, indicating the denaturation of TWIPNs during the heating process. The heat treatment promoted the expansion and reconstruction of TWIPN aggregates. As previously reported, heat treatment results in an increase in α-helices and β-turns and a decrease in β-sheets and random coils, verifying that molecular chains are partially folded to form aggregates under heat treatment (Sun et al., 2016).

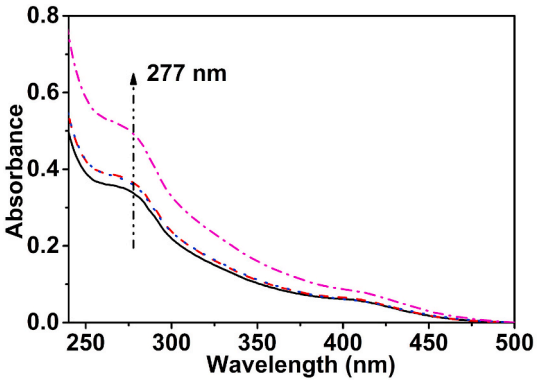

Fig. 2. Ultraviolet absorption spectra of tea water-insoluble protein nanoparticle suspension at different temperatures. (—— , Unheated; — –, 60 °C; • • • •, 100 °C; – · –, 120 °C.)

3.1.5. AFM analysis of TWIPNs

The microstructure plays an important part in the micro characteristics of proteins (Luo, Zhang, Wu, Liang, & Li, 2020; Zhou & Yang, 2019). AFM has been applied extensively to image proteins (Ren, Chen, Zhang, Lin, & Li, 2019; Sow, Toh, Wong, & Yang, 2019). The AFM scanning images of TWIPNs heated at different temperatures are shown in Fig. 3. The height of the unheated TWIPNs was roughly 35 nm with a mainly rough and non-homogeneous morphology according to the analysis based on the graph. Particles were gathered from each other (Fig. 3A and A').

After heating at 60 °C, the height of TWIPNs decreased to 20 nm and their size decreased markedly. TWIPNs became smaller and aggregation of TWIPNs decreased (Fig. 3B and B'). The roughness and sharpness of TWIPNs heated at 100 °C reduced compared with those treated at 60 °C (Fig. 3C and C'). The height of TWIPNs heated at 120 °C was consistent with those unheated and heated at 100 °C. Further aggregation of TWIPNs was noted and their shape was irregular, as shown in Fig. 3D and D'. These observations showed that a low temperature like 60 °C could reduce the particle size of TWIPNs. However, TWIPNs heated at high temperatures such as 100 °C and 120 °C tended to rebuild aggregates. Protein aggregation after heating was also found in the previous report (Vate & Benjakul, 2016). Proteins heated at low and high temperatures would unfold and aggregate again like zeins; however, in most cases, the aggregated proteins could not recover the initial structure, especially after the high-temperature treatment (Sun et al., 2016).

3.2. Characteristics of TWIPNPEs

3.2.1. Particle size distribution of TWIPNPEs

Numerous studies have reported that heat treatment of proteins can change the emulsion properties (Keerati, 2009; Makeri et al., 2019; Wang et al., 2019). The particle size distribution and $d_{4,3}$ are used to characteristics of Pickering emulsions (Sedaghat Doost et al., 2019). First, the particle size distribution and $d_{4,3}$ of TWIPNPEs stabilized by TWIPNs under different heat treatments in a water system were determined (Fig. 4). The range of particle size distribution of TWIPNPEs stabilized using heat-treated TWIPNs decreased with the increase in TWIPN concentration. The particle size distribution of the Pickering emulsions stabilized using heated TWIPNs above 10 g/L showed two peaks between 1 and 10 μm (Fig. 4A–C). The volume fraction of Pickering emulsions increased in peak 1 and decreased in peak 2 as the TWIPN concentration increased, indicating that the size of emulsion droplets decreased with the increase in the TWIPN concentrations.

The particle size distribution of TWIPNPEs prepared using heat-treated TWIPNs in a water system showed similar changes with increasing TWIPN concentrations, compared with those stabilized using unheated TWIPNs as a previous report (Ren, Chen, Zhang, Lin, & Li,

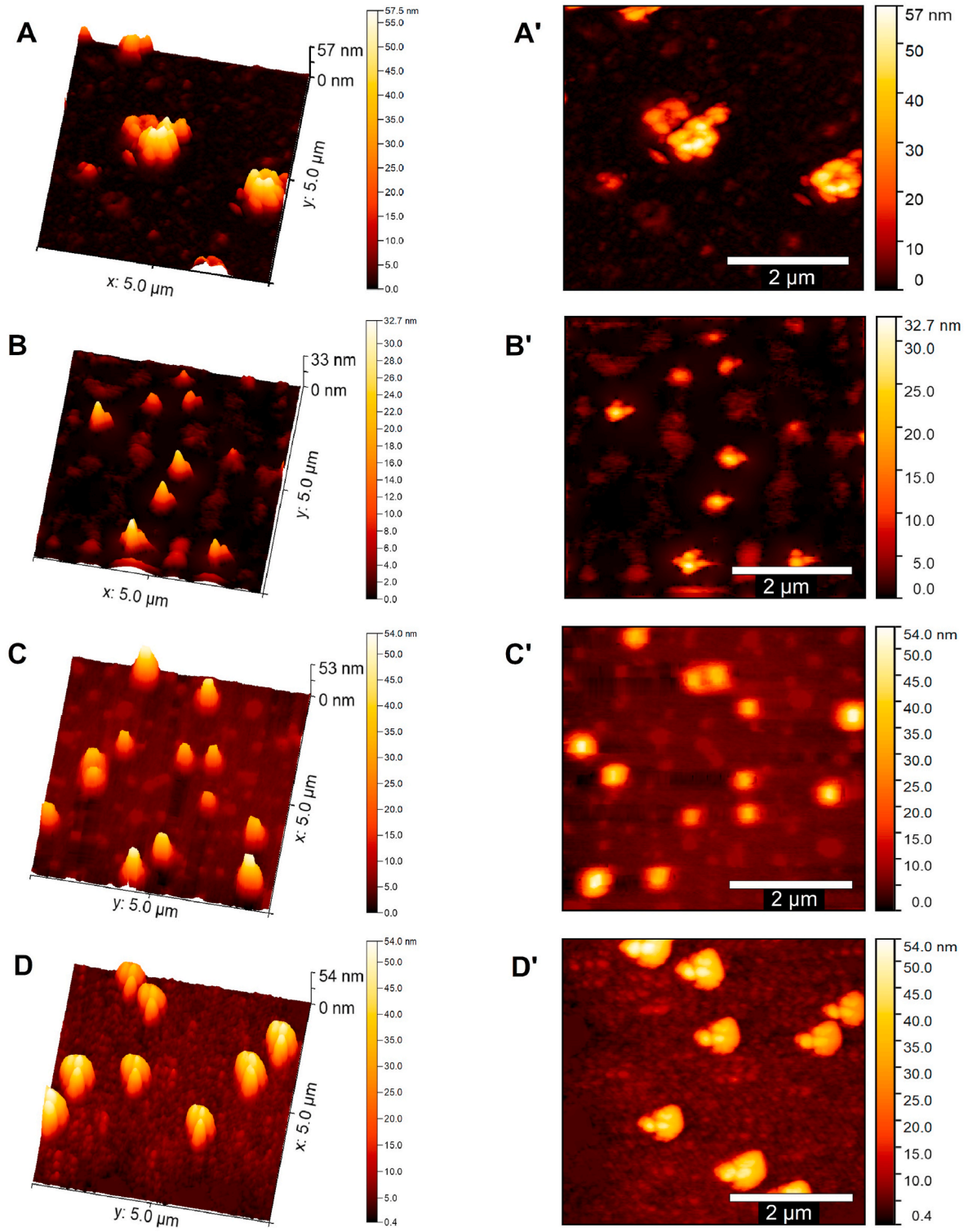

Fig. 3. Top view (A-D) and 3D-view (A'-D') atomic force microscopy images of tea water-insoluble protein nanoparticles treated at different temperatures. (A and A', unheated; B and B', 60 °C; C and C', 100 °C; D and D', 120 °C.)

2019). The particle size distribution of TWIPNPEs prepared using TWIPNs (5 g/L) heated at 60, 100 and 120 °C changed from a bimodal peak to a unimodal peak. Meanwhile, the particle size distribution range changed from 20 to 200 to 100–400 μm.

With increasing temperature, the volume fraction of TWIPNPEs decreased in peak 1 and increased in peak 2, showing that the size of the emulsion droplets became larger with an increase in temperature. The particle size distribution of TWIPNPEs prepared using heat-treated TWIPNs in a 10 g/L SDS system showed a similar change to those in the water system (Fig. S1). This was mainly attributed to the change in the TWIPN structure under heat treatment according to FTIR analysis. Proteins can be expanded and refolded into β-sheets; meanwhile, random coils are transformed into α-helices (Subirade, Kelly, Guéguen & Pézolet, 1998). This result can be attributed that the molecule chain of TWIPNs was partially folded and aggregated. Heat treatment could lead to the expansion and transformation of heat-treated TWIPN structures,

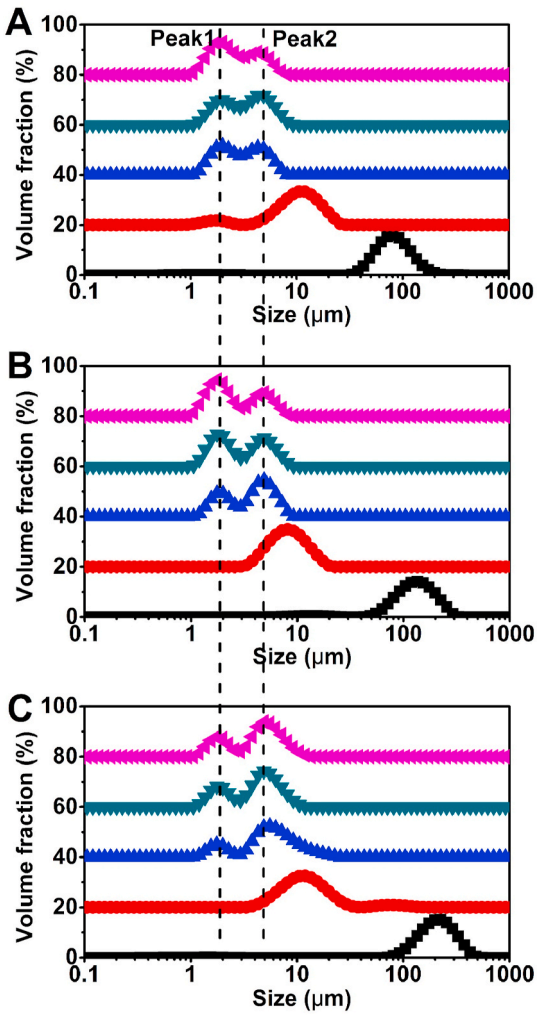

Fig. 4. Particle size distribution (A, B and C) of Pickering emulsions prepared using heat-treated tea water-insoluble protein nanoparticles. (■, 5 g/L; ●, 10 g/L; ▲, 20 g/L; ▼, 30 g/L; ◀, 40 g/L; A, 60 °C; B, 100 °C; C, 120 °C. The suspension phase is deionized water.)

which were not easily adsorbed at the oil and water interface, leading to the instability of emulsions (Raikos, 2010). Furthermore, the optical microscopy observation of fresh TWIPNPEs constructed from TWIPNs treated at different temperatures was consistent with the results of the $d_{4,3}$ and particle size distribution (Fig. 5). The droplets of TWIPNPEs could be observed clearly. The flocculation between the emulsion droplets was obvious, especially for Pickering emulsions stabilized using TWIPNs (10 g/L).

3.2.2. *Flocculation index of TWIPNPEs*

To further analyze the effect of heat treatment of TWIPNs on the flocculation of Pickering emulsions, the FI of TWIPNPEs prepared using heat-treated TWIPNs is shown in Table 2. At a low TWIPN concentration of 5 g/L, the FI of TWIPNPEs decreased at 60 °C and then increased at 100 and 120 °C. At the TWIPN concentration of 10 g/L, the flocculation did not appear at 60 and 100 °C and the FI of TWIPNPEs was very little at 120 °C. This result can be attributed to that insufficient particles cannot cover the full droplet surface to lead to the flocculation of emulsion droplets, but emulsion droplets were not or very little flocculated when the number of particles was a lot enough (Ren, Chen, Zhang, Lin, & Li, 2019). At a high TWIPN concentration of 40 g/L, the FI of TWIPNPEs using TWIPNs heated at 100 and 120 °C increased compared with those prepared using unheated TWIPNs as previously reported (Ren et al., 2020). Moderate heat treatment is beneficial to reduce the FI of TWIPNPEs at a low TWIPN concentration. However, high temperatures, such as 100 and 120 °C, accelerated the flocculation of emulsion droplets, particularly at high protein concentrations. Non-adsorbed proteins at high concentrations boosted the flocculation of emulsion droplets through depletion destabilization, even causing droplet coalescence (Yan et al., 2020). At a high TWIPN concentration of 40 g/L, the FI of TWIPNPEs prepared using heat-treated TWIPNs was higher than that of TWIPNPEs prepared using unheated TWIPNs as previously reported (Ren et al., 2020). This indicated that a high TWIPN concentration (40 g/L) promoted the flocculation of TWIPNPEs in accordance with the results of the microscopic observation (Fig. 5). These results indicated that the flocculation levels were associated with the TWIPN concentration and heat treatment temperature, similar to previous reports (Ren, Chen, Zhang, Lin, & Li, 2019; Sarkar et al., 2016).

3.2.3. *Creaming index of TWIPNPEs*

The effect of the different heat-treated TWIPNs on the stability of

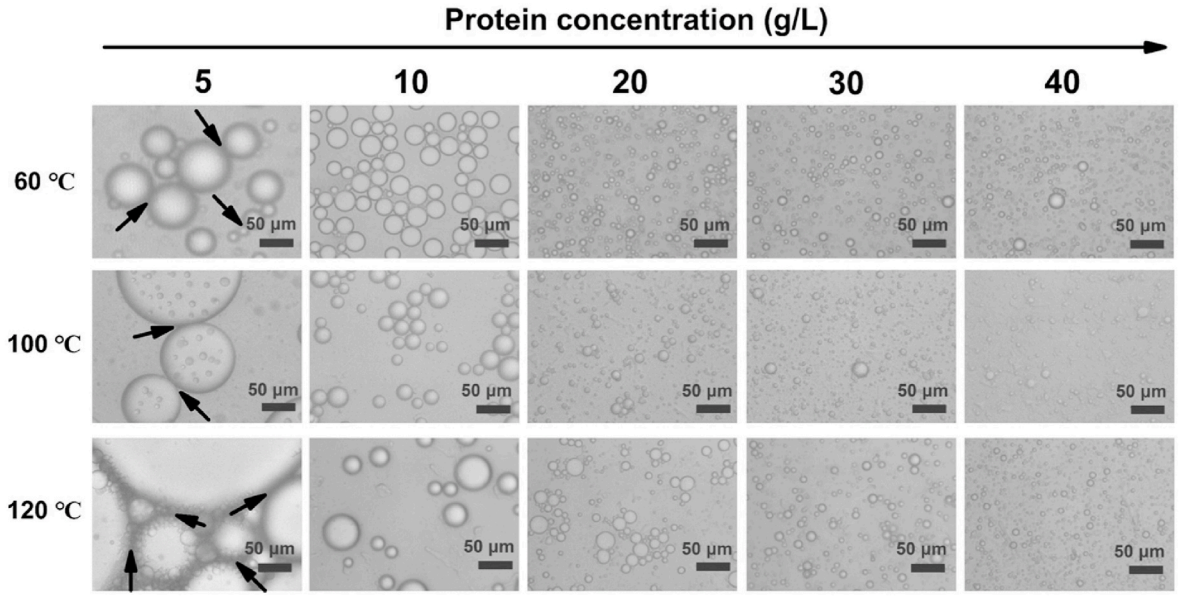

Fig. 5. Microscopic observation of fresh Pickering emulsions prepared using heat-treated tea water-insoluble protein nanoparticles.

Table 2
Flocculation index of Pickering emulsions prepared using heat-treated tea water-insoluble protein nanoparticles.

Treatment	Protein concentration (g/L)	$d_{4,3}$ (μm)		Flocculation index (%)
		Water	SDS	
60 °C	5	85.86 ± 0.13[a]	81.24 ± 0.67[a]	5.69 ± 0.68
	10	10.76 ± 0.03[b]	18.86 ± 0.51[b]	–
	20	3.26 ± 0.01[d]	2.86 ± 0.01[c]	13.89 ± 0.05
	30	3.57 ± 0.00[c]	2.96 ± 0.01[c]	20.48 ± 0.33
	40	2.98 ± 0.00[e]	2.34 ± 0.01[c]	27.00 ± 0.25
100 °C	5	134.67 ± 2.52[a]	107.33 ± 1.53[a]	25.47 ± 2.70
	10	8.66 ± 0.06[b]	11.90 ± 1.61[b]	–
	20	3.87 ± 0.01[c]	3.68 ± 0.01[c]	5.16 ± 0.53
	30	3.38 ± 0.01[c]	3.15 ± 0.02[c]	7.52 ± 0.32
	40	3.04 ± 0.01[c]	2.50 ± 0.01[c]	21.30 ± 0.00
120 °C	5	214.00 ± 19.67[a]	141.33 ± 8.08[a]	51.42 ± 0.30
	10	15.53 ± 0.32[b]	15.30 ± 0.20[b]	1.53 ± 3.27
	20	6.26 ± 0.03[c]	4.20 ± 0.03[c]	49.17 ± 0.00
	30	4.36 ± 0.01[d]	3.52 ± 0.02[c]	23.75 ± 0.00
	40	4.57 ± 0.01[d]	3.04 ± 0.01[c]	50.33 ± 0.00

* The $d_{4,3}$ and FI represent the size of the emulsion droplets and flocculation index, respectively. Different lowercase letters denote significant differences ($P < 0.05$) at the same temperature. Values are given as means ± SD from triplicate tests.

TWIPNPEs was further determined. CI is a usual index for the stability of emulsions (Li, Fu, et al., 2020). The CI changes of TWIPNPEs with storage time are shown in Fig. 6. The CI of TWIPNPEs stabilized using TWIPNs heated at the same temperature decreased with increasing TWIPN concentrations. As previously reported, increasing the TWIPN concentration within a certain range favored the storage stability of TWIPNPEs (Ren, Chen, Zhang, Lin, & Li, 2019).

The CI changes of TWIPNPEs prepared using TWIPNs heated at 60 °C with storage time are shown in Fig. 6A. During storage for 50 days, TWIPNPEs prepared using heat-treated TWIPNs at 5 and 10 g/L reached a stable CI value after storage of 5 days. At a TWIPN concentration of 20 g/L, creaming was not found in 5 days. No creaming of TWIPNPEs prepared using TWIPN at concentrations of 3.0 and 40 g/L was observed during the storage time (Fig. 6A). The CI of TWIPNPEs prepared using heated TWIPNs decreased with increasing TWIPN concentrations (Fig. 6A, B and C). The oils in TWIPNPEs prepared using 5 g/L TWIPN heated at 120 °C spilled over at the top of the tube after 4 h, indicating the internal phase separation; therefore, no data were recorded. Besides, the CI of TWIPNPEs stabilized using the same TWIPN concentration changed differently as the temperature increased (Table S3). These results could be observed using images in Fig. 6. Heat treatment at 60 °C reduced the size of TWIPNs to stabilize TWIPNPEs compared with that of TWIPNPEs prepared using unheated TWIPNs as a previous report (Ren et al., 2020).

However, TWIPNPEs stabilized using TWIPNs heated at 100 and 120 °C did not form stable emulsions. Creaming of TWIPNPEs stabilized by TWIPNs heated at 100 °C appeared after 25 days. TWIPNPEs stabilized using TWIPN concentrations of 30 and 40 g/L heated at 120 °C began to show creaming after 5 and 20 days, respectively. The increase in the particle size of TWIPNs (30 and 40 g/L) and the flocculation level at 100 and 120 °C led to the decrease of emulsion stability. These results indicated that TWIPNs were unevenly distributed and aggregated at the oil-water interface, which reduced the stability of the emulsion droplets and eventually led to the instability of TWIPNPEs. As previously reported, the interactions between protein particles could be responsible for increasing creaming when protein particles were heated (Raikos, 2010).

According to the above analysis, the heat treatment of TWIPNs reduced the stability of TWIPNPEs. A schematic diagram of the stability of TWIPNPEs prepared using heat-treated TWIPNs was proposed and shown in Fig. 7. TWIPNs differed from the water-soluble proteins like soy protein isolates, which can be modified using heat treatment as Pickering stabilizers to exhibit better emulsifying properties compared with the unheated soy protein isolates (Liu & Tang, 2016). Apart from changes in structures, the intermolecular forces of TWIPNs changed under heat treatment (Table 1). In addition, the intermolecular forces maintained by disulfide bonds are strong compared with those of non-covalent bonds (Liu & Tang, 2016). This indicated that the forces acting on TWIPNs changed at high temperatures like 100 and 120 °C, resulting in the structural rearrangements and enhancement of the intermolecular forces. Ultimately TWIPNPEs were unstable due to the aggregation of TWIPNs at the surface of different emulsion droplets.

3.3. Rheological behavior of TWIPNPEs

The interactions of the adsorbed proteins at the surface of the emulsion droplets or between the droplets affect the viscosity of emulsions. The apparent viscosity of TWIPNPEs prepared using heat-treated TWIPNs is shown in Fig. 8. The range of 0.1–10 s^{-1} was the pseudoplastic region and the range of 10–100 s^{-1} was the second Newton zone (Fig. 8A–D). The apparent viscosity of TWIPNPEs prepared using heat-treated TWIPNs showed a decreasing trend at 0.1–100 s^{-1}, indicating the shear-thinning behavior of TWIPNPEs prepared using heat-treated TWIPNs with increasing the shear rate. The shear-thinning behavior of emulsions can be attributed to the break-up of flocculation or aggregates of TWIPNs at the oil and water interface with the increase in shear rate (Dybowska, 2011).

Besides, the apparent viscosities of TWIPNPEs prepared using heat-treated TWIPN concentrations of 5, 10 and 20 g/L (Fig. 8B, C and D) were higher than those prepared using unheated TWIPNs at the same concentration (Fig. 8A). However, the apparent viscosities of TWIPNPEs prepared using heat-treated TWIPN concentrations of 30 and 40 g/L decreased at the same shear rate compared to those prepared using unheated TWIPNs. These results were suggested that the interaction between emulsion droplets or TWIPN molecules was damaged to different extents after shearing and heat treatment led to the changes in the structure of TWIPNs at different temperatures. According to the above results of TWIPN characteristics, TWIPNs could be aggregated between the TWIPN particles after heated at 100 and 120 °C as shown in Fig. 3. The apparent viscosities of TWIPNPEs prepared using heat-treated TWIPNs (30 and 40 g/L) at 100 and 120 °C was higher than those at 60 °C. This result can be due to that the formation of bridges between the droplets, as well as the existence of droplets with larger aggregates at the oil and water interface, would increase the emulsion viscosity (Keerati, 2009).

To explore the changes in viscoelasticity of TWIPNPEs prepared using different heated TWIPNs, the viscoelasticity of the fresh TWIPNPEs prepared using the TWIPN concentration of 20 g/L is presented in Fig. 9. The G′ and G″ value of TWIPNPEs decreased with the increase in temperatures at the same angular rate (Fig. 9A). The G′

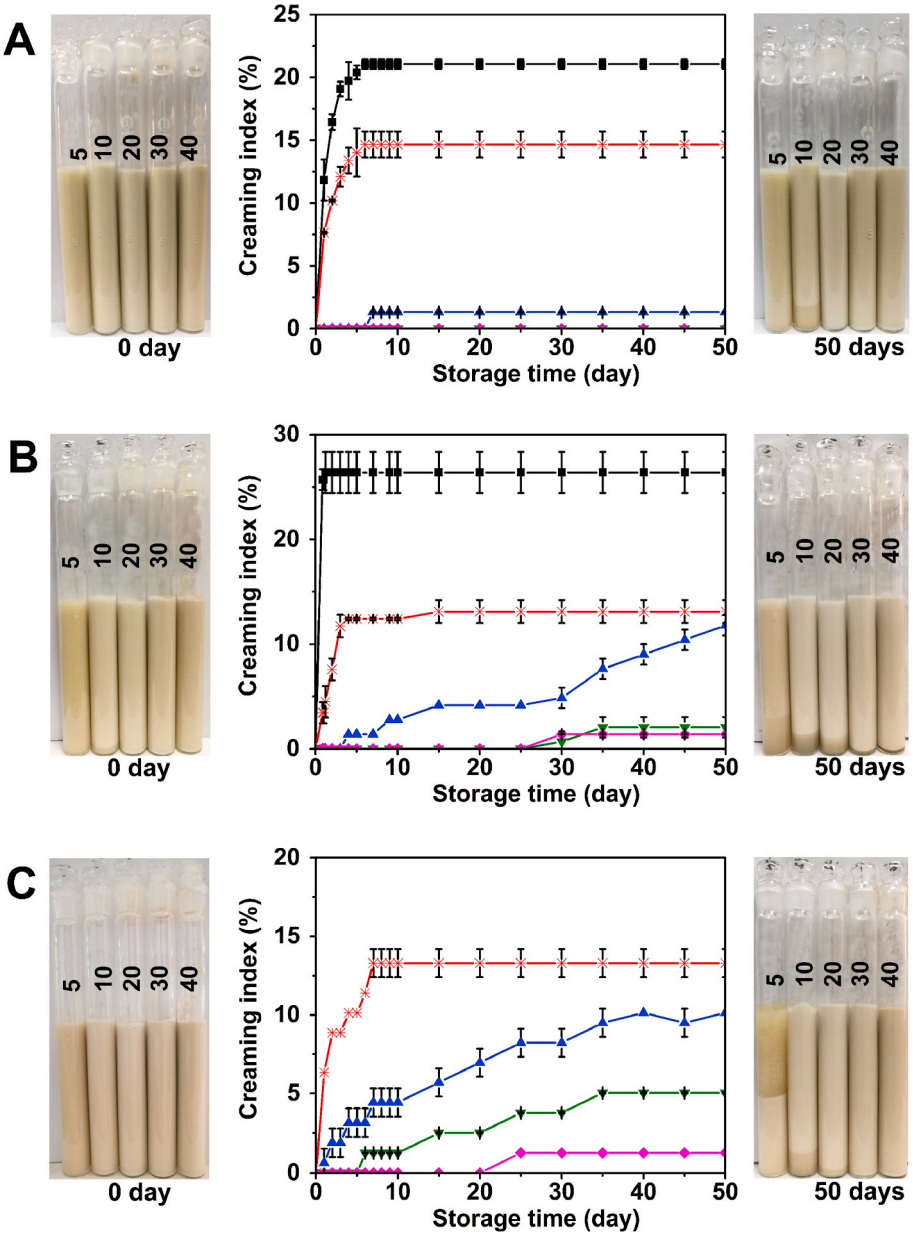

Fig. 6. Creaming index of Pickering emulsions prepared using heat-treated tea water-insoluble protein nanoparticles during the storage of 50 d. (■, 5 g/L; ∗, 10 g/L; ▲, 20 g/L; ▼, 30 g/L; ◆, 40 g/L; A, 60 °C; B, 100 °C; C, 120 °C.).
* Values are given as means ± SD from triplicate tests.

values of TWIPNPEs prepared using different heated TWIPNs at 60 and 100 °C were greater than the G″ values, which indicated the gel-like characteristics of TWIPNPEs as a previous report (Ren et al., 2020). The flocculation between the droplets increased the viscoelasticity of TWIPNPEs prepared using different heated TWIPNs at a concentration of 20 g/L to a certain extent (Table 2). The viscoelasticity of TWIPNPEs prepared using TWIPNs heated at 120 °C decreased, showing the gel-like characteristics within the range of 0.1–80 rad/s. However, a higher G″ value than G′ value appeared after 80 rad/s, indicating that the gel-like structure of TWIPNPEs was destroyed. The viscoelasticity of TWIPNPEs was reduced after the high-temperature treatment of TWIPNs, which was related to the viscosity. According to a previous report, the low viscosity is not helpful for the gel-like behavior of emulsions (Lee, Chan, & Ali, 2012).

Finally, the loss coefficient of TWIPNPEs was further analyzed at different angular rates (Fig. 9B). All the loss coefficients of the emulsions were less than one below 80 rad/s and they increased with the increase in temperatures at the same angular rate, indicating that the elasticity of TWIPNPEs decreased relatively. This result was consistent with the G′ and G″ values of TWIPNPEs as shown in Fig. 9A. However, the loss coefficient of TWIPNPEs prepared using TWIPNs heated at 120 °C, was not apparent at an angular rate above 80 rad/s. This could be due to that the elasticity of TWIPNPEs decreased sharply under these conditions and heat-treated TWIPNs could not be effectively adsorbed at the oil-water interface to stabilize TWIPNPEs, resulting in the instability of TWIPNPEs.

4. Conclusion

The characteristics of heat-treated TWIPNs were reported. The noncovalent bonds, as well as disulfide bonds, participated in the interaction forces between the heat-treated TWIPNs, indicating that

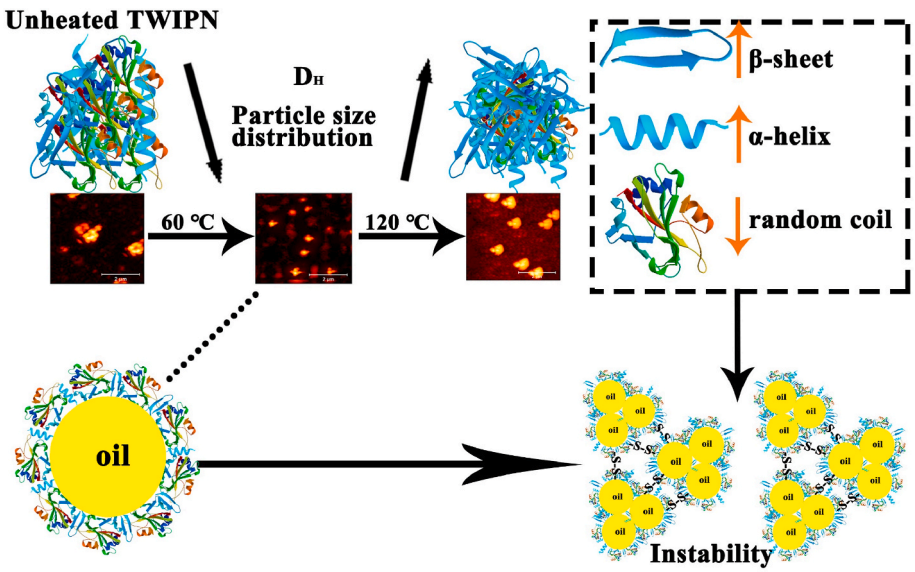

Fig. 7. Schematic diagram of the change of Pickering emulsions prepared using heat-treated tea water-insoluble protein nanoparticles.

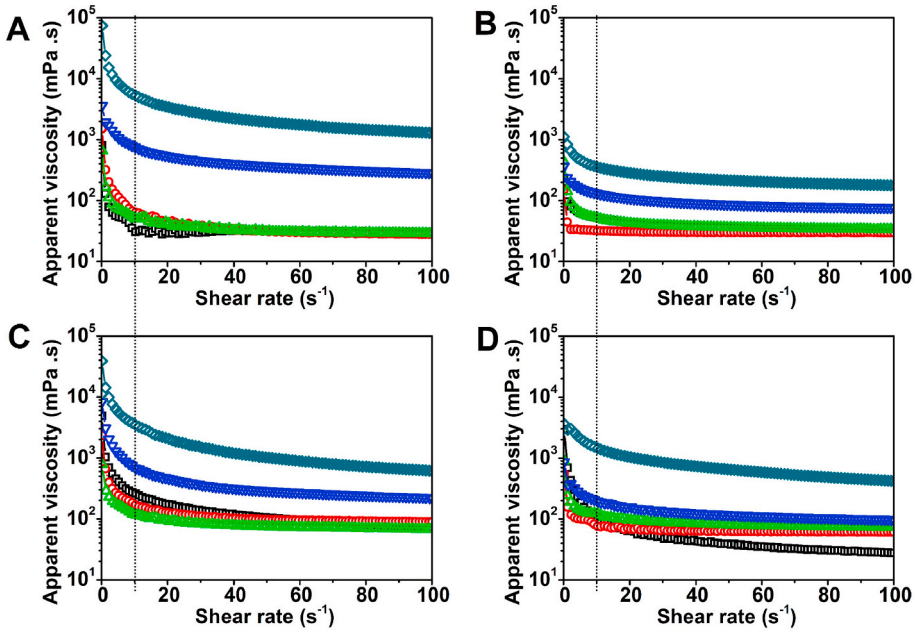

Fig. 8. Change of the apparent viscosity of Pickering emulsions prepared using heat-treated tea water-insoluble protein nanoparticles at shear rates of 0.1-100 s^{-1}. (□, 5 g/L; ◆, 10 g/L; ○,20 g/L; ▽, 30 g/L; ◇, 40 g/L; A, Unheated; B, 60 °C; C, 100 °C; D, 120 °C.)

disulfide bonds and noncovalent bonds synergistically participated in the intermolecular forces of heat-treated TWIPNs. Besides, heat treatment promoted the expansion and reconstruction of TWIPNs due to that the random coil contents decreased and the contents of α-helices and β-sheets increased with the increase in temperature. These results were important for exhibiting the characteristics of Pickering emulsions prepared by TWIPNs. The particle size distribution of Pickering emulsions prepared using TWIPNs (5 g/L) heated at 60, 100 and 120 °C changed from a bimodal peak to a unimodal peak. A possible mechanism was proposed to indicate the instability of Pickering emulsions using TWIPNs heated at high temperatures due to the flocculation of Pickering emulsions. High temperature led to the decrease of the apparent viscosity and gel-like behavior of Pickering emulsions prepared using heat-treated TWIPNs. This work helps utilize TWIPNs treated at different temperatures from tea residues for constructing food-grade Pickering emulsions in food industry.

CRediT authorship contribution statement

Zhongyang Ren: Data curation, Formal analysis, Investigation, Methodology, Resources, Software, Validation, Visualization, Writing – original draft. **Zhongzheng Chen:** Data curation, Formal analysis, Writing – original draft. **Yuanyuan Zhang:** Data curation, Formal analysis, Methodology. **Xiaorong Lin:** Validation, Visualization, Writing – original draft. **Zhanming Li:** Visualization. **Wuyin Weng:** Formal analysis, Writing – review & editing. **Hongshun Yang:** Conceptualization, Funding acquisition, Project administration, Supervision, Writing – review & editing. **Bin Li:** Funding acquisition, Project administration, Supervision, Writing – review & editing.

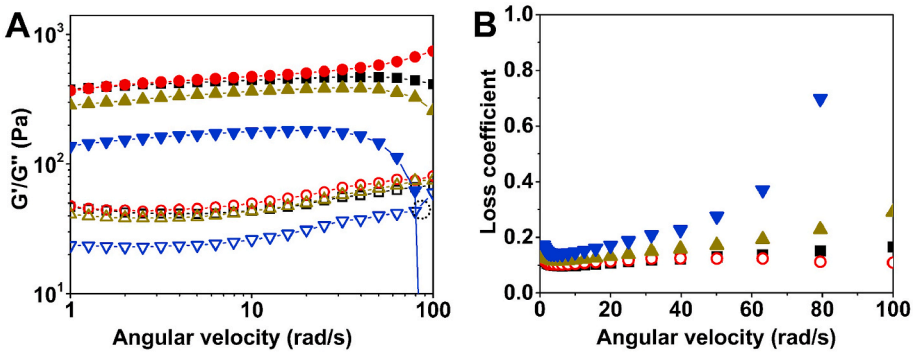

Fig. 9. Viscoelastic parameters of fresh Pickering emulsions prepared using heat-treated tea water-insoluble protein nanoparticles at angular velocities of 0.1-100 rad/s. (A (G'/G"): ■, G' Unheated; ●, G' 60 °C; ▲, G' 100 °C; ▼, G' 120 °C; □, G" Unheated; ○, G" 60 °C; △,G" 100 °C; ▽, G" 120 °C. B (Loss coefficient): ■, Unheated; ○, 60 °C; ▲, 100 °C; ▼, 120 °C.). * G' and G" represent storage modulus and loss storage, respectively.

Declaration of competing interest

We declare that we have no commercial or associative interest that represents a conflict of interest in connection with this manuscript. We have no financial and personal relationships with other people or organizations that can inappropriately influence our work.

Acknowledgement

We thank Shenzhen Shenbao Huacheng Tech. Co., Ltd., for kindly providing the tea leaves. This study was funded by the Special Fund from the Modern Agricultural Industry of China (CARS-19), Research Initial Fund from Jimei University (ZQ2020011), Natural Science Foundation of Jiangsu Province (BK20181184) and Singapore Ministry of Education Academic Research Fund Tier 1 (R-160-000-A40-114).

Appendix A. Supplementary data

Supplementary data to this article can be found online at https://doi.org/10.1016/j.lwt.2021.111999.

References

Ananey-Obiri, D., Matthews, L., Azahrani, M. H., Ibrahim, S. A., Galanakis, C. M., & Tahergorabi, R. (2018). Application of protein-based edible coatings for fat uptake reduction in deep-fat fried foods with an emphasis on muscle food proteins. *Trends in Food Science & Technology, 80*, 167–174.

Baltacıoğlu, H., Bayındırlı, A., Severcan, M., & Severcan, F. (2015). Effect of thermal treatment on secondary structure and conformational change of mushroom polyphenol oxidase (PPO) as food quality related enzyme: A FTIR study. *Food Chemistry, 187*, 263–269.

Carbonaro, M., & Nucara, A. (2010). Secondary structure of food proteins by Fourier transform spectroscopy in the mid-infrared region. *Amino Acids, 38*, 679–690.

Chen, B., Huang, J., Liu, Y., Liu, H., Zhao, Y., & Wang, J. J. (2021). Effects of the curcumin-mediated photodynamic inactivation on the quality of cooked oysters with Vibrio parahaemolyticus during storage at different temperature. *International Journal of Food Microbiology, 345*, 109152.

Chen, X., McClements, D. J., Wang, J., Zou, L., Deng, S., Liu, W., et al. (2018a). Coencapsulation of (-)-epigallocatechin-3-gallate and quercetin in particle-stabilized W/O/W emulsion gels: Controlled release and bioaccessibility. *Journal of Agricultural and Food Chemistry, 66*, 3691–3699.

Chen, L., Zhou, Y., He, Z., Liu, Q., Lai, S., & Yang, H. (2018b). Effect of exogenous ATP on the postharvest properties and pectin degradation of mung bean sprouts (*Vigna radiata*). *Food Chemistry, 251*, 9–17.

Chevalier, Y., & Bolzinger, M. A. (2013). Emulsions stabilized with solid nanoparticles: Pickering emulsions. *Colloids and Surfaces A: Physicochemical and Engineering Aspects, 439*, 23–34.

Dybowska, B. E. (2011). Whey protein-stabilized emulsion properties in relation to thermal modification of the continuous phase. *Journal of Food Engineering, 104*, 81–88.

Emmambux, M. N., & Taylor, J. R. N. (2009). Properties of heat-treated sorghum and maize meal and their prolamin proteins. *Journal of Agricultural and Food Chemistry, 57*, 1045–1050.

Ho, Q. T., Murphy, K. M., Drapala, K. P., O Callaghan, T. F., Fenelon, M. A., O Mahony, J. A., et al. (2018). Effect of pH and heat treatment on viscosity and heat coagulation properties of milk protein concentrate. *International Dairy Journal, 85*, 219–224.

Keerati, M. (2009). Heat-induced changes in oil-in-water emulsions stabilized with soy protein isolate. *Food Hydrocolloids, 23*, 2141–2148.

Lee, M. N., Chan, H. K., & Ali, M. (2012). Characteristics of Pickering emulsion gels formed by droplet bridging. *Langmuir, 28*, 3085–3091.

Liang, H. N., & Tang, C. H. (2014). Pea protein exhibits a novel Pickering stabilization for oil-in-water emulsions at pH 3.0. *LWT-Food Science and Technology, 58*, 463–469.

Li, Y., Bai, Y., Huang, J., Yuan, C., Ding, T., Liu, D., et al. (2020a). Airglow discharge plasma treatment affects the surface structure and physical properties of zein films. *Journal of Food Engineering, 273*, 109813.

Li, K., Fu, L., Zhao, Y., Xue, S., Wang, P., Xu, X., et al. (2020b). Use of high-intensity ultrasound to improve emulsifying properties of chicken myofibrillar protein and enhance the rheological properties and stability of the emulsion. *Food Hydrocolloids, 98*, 105275.

Liu, X., Liu, Y., Guo, J., Yin, S., & Yang, X. (2017). Microfluidization initiated cross-linking of gliadin particles for structured algal oil emulsions. *Food Hydrocolloids, 73*, 153–161.

Liu, F., & Tang, C. H. (2013). Soy protein nanoparticle aggregates as Pickering stabilizers for oil-in-water emulsions. *Journal of Agricultural and Food Chemistry, 61*, 8888–8898.

Liu, F., & Tang, C. H. (2016). Soy glycinin as food-grade Pickering stabilizers: Part. I. Structural characteristics, emulsifying properties and adsorption/arrangement at interface. *Food Hydrocolloids, 60*, 606–619.

Luo, Y., Zhang, Y., Wu, J., Liang, L., & Li, Y. (2020). Nanotechnology with biological macromolecules. *International Journal of Biological Macromolecules, 155*, 834.

Makeri, M., Muhammad, K., Ghazali, H., & Mohammed, A. (2019). Influence of temperature and ionic conditions on the rheology and droplets characteristics of winged bean protein stabilized oil-in-water emulsion. *Journal of Food Measurement and Characterization, 13*, 97–106.

Millqvist-Fureby, A., Elofsson, U., & Bergenståhl, B. (2001). Surface composition of spray-dried milk protein-stabilised emulsions in relation to pre-heat treatment of proteins. *Colloids and Surfaces B: Biointerfaces, 21*, 47–58.

Nikbakht Nasrabadi, M., Sedaghat Doost, A., Goli, S. A. H., & Van der Meeren, P. (2020). Effect of thymol and Pickering stabilization on *in-vitro* digestion fate and oxidation stability of plant-derived flaxseed oil emulsions. *Food Chemistry, 311*, 125872.

Ning, F., Ge, Z., Qiu, L., Wang, X., Luo, L., Xiong, H., et al. (2020). Double-induced Se-enriched peanut protein nanoparticles preparation, characterization and stabilized food-grade Pickering emulsions. *Food Hydrocolloids, 99*, 105308.

Raikos, V. (2010). Effect of heat treatment on milk protein functionality at emulsion interfaces. A review. *Food Hydrocolloids, 24*, 259–265.

Ren, Z., Chen, Z., Zhang, Y., Lin, X., & Li, B. (2019). Novel food-grade Pickering emulsions stabilized by tea water-insoluble protein nanoparticles from tea residues. *Food Hydrocolloids, 96*, 322–330.

Ren, Z., Chen, Z., Zhang, Y., Lin, X., & Li, B. (2020). Characteristics and rheological behavior of Pickering emulsions stabilized by tea water-insoluble protein nanoparticles via high-pressure homogenization. *International Journal of Biological Macromolecules, 151*, 247–256.

Ren, Z., Chen, Z., Zhang, Y., Zhao, T., Ye, X., Gao, X., et al. (2019). Functional properties and structural profiles of water-insoluble proteins from three types of tea residues. *LWT-Food Science and Technology, 110*, 324–331.

Ren, Z., Li, Z., Chen, Z., Zhang, Y., Lin, X., Weng, W., et al. (2021). Characteristics and application of fish oil-in-water pickering emulsions structured with tea water-insoluble proteins/κ-carrageenan complexes. *Food Hydrocolloids, 114*, 106562.

Sarkar, A., Murray, B., Holmes, M., Ettelaie, R., Abdalla, A., & Yang, X. (2016). In vitro digestion of pickering emulsions stabilized by soft whey protein microgel particles: Influence of thermal treatment. *Soft Matter, 12*, 3558–3569.

Schmitt, C., Moitzi, C., Bovay, C., Rouvet, M., Bovetto, L., Donato, L., et al. (2010). Interal structure and colloidal behaviour of covalent whey protein microgels obtained by heat treatment. *Soft Matter, 6*, 4876–4884.

Sedaghat Doost, A., Nikbakht Nasrabadi, M., Kassozi, V., Dewettinck, K., Stevens, C. V., & Van der Meeren, P. (2019). Pickering stabilization of thymol through green emulsification using soluble fraction of almond gum-Whey protein isolate nano-complexes. *Food Hydrocolloids, 88*, 218–227.

Shen, L. L., Zhu, Q. Q., Huang, F. W., Xu, H., Wu, X. L., Xiao, H. F., et al. (2015). Effect of heat treatment on structure and immunogenicity of recombinant peanut protein Ara h 2.01. *LWT-Food Science and Technology, 60*, 964–969.

Sow, L. C., Chong, J. M. N., Xu, L., & Yang, H. (2018). Effects of κ-carrageenan on the structure and rheological properties of fish gelatin. *Journal of Food Engineering, 239*, 92–103.

Sow, L. C., Tan, S. J., & Yang, H. (2019). Rheological properties and structure modification in liquid and gel of tilapia skin gelatin by the addition of low acyl gellan. *Food Hydrocolloids, 90*, 9–18.

Sow, L. C., Toh, N. Z. Y., Wong, C. W., & Yang, H. (2019). Combination of sodium alginate with tilapia fish gelatin for improved texture properties and nanostructure modification. *Food Hydrocolloids, 94*, 459–467.

Subirade, M., Kelly, I., Guéguen, J., & Pézolet, M. (1998). Molecular basis of film formation from a soybean protein: Comparison between the conformation of glycinin in aqueous solution and in films. *International Journal of Biological Macromolecules, 23*, 241–249.

Sun, C., Lei, D., He, X., Liu, F., Fang, Y., & Gao, Y. (2016). Effect of heat treatment on physical, structural, thermal and morphological characteristics of zein in ethanol-water solution. *Food Hydrocolloids, 58*, 11–19.

Tan, J., Martini, S., Wang, Y., Kong, F., Hartel, R., Barbosa-Cánovas, G., et al. (2019). Interlaboratory measurement of rheological properties of tomato salad dressing. *Journal of Food Science, 84*, 3204–3212.

Tong, P., Gao, J., Chen, H., Li, X., Zhang, Y., Jian, S., et al. (2012). Effect of heat treatment on the potential allergenicity and conformational structure of egg allergen ovotransferrin. *Food Chemistry, 131*, 603–610.

Vate, N. K., & Benjakul, S. (2016). Combined effect of squid ink tyrosinase and tannic acid on heat induced aggregation of natural actomyosin from sardine. *Food Hydrocolloids, 56*, 62–70.

Wada, R., Fujita, Y., & Kitabatake, N. (2006). Effects of heating at neutral and acid pH on the structure of beta-lactoglobulin a revealed by differential scanning calorimetry and circular dichroism spectroscopy. *Biochimica et Biophysica Acta, 1760*, 841–847.

Wang, M., Chen, X., Guo, J., Yang, J., Wang, J., & Yang, X. (2019). Stabilization of foam and emulsion by subcritical water-treated soy protein: Effect of aggregation state. *Food Hydrocolloids, 87*, 619–628.

Wu, J., Shi, M., Li, W., Zhao, L., Wang, Z., Yan, X., et al. (2015). Pickering emulsions stabilized by whey protein nanoparticles prepared by thermal cross-linking. *Colloids and Surfaces B: Biointerfaces, 127*, 96–104.

Xiao, J., Wang, X., Gonzalez, A. J. P., & Huang, Q. (2016). Kafirin nanoparticles-stabilized Pickering emulsions: Microstructure and rheological behavior. *Food Hydrocolloids, 54*, 30–39.

Xue, J., Wang, T., Hu, Q., Zhou, M., & Luo, Y. (2018). Insight into natural biopolymer-emulsified solid lipid nanoparticles for encapsulation of curcumin: Effect of loading methods. *Food Hydrocolloids, 79*, 110–116.

Yan, X., Ma, C., Cui, F., McClements, D. J., Liu, X., & Liu, F. (2020). Protein-stabilized Pickering emulsions: Formation, stability, properties, and applications in foods. *Trends in Food Science & Technology, 103*, 293–303.

Zhou, Y., & Yang, H. (2019). Effects of calcium ion on gel properties and gelation of tilapia (*Oreochromis niloticus*) protein isolates processed with pH shift method. *Food Chemistry, 277*, 327–335.

Zhou, F., Yan, L., Yin, S., Tang, C., & Yang, X. (2018). Development of Pickering emulsions stabilized by gliadin/proanthocyanidins hybrid particles (GPHPs) and the fate of lipid oxidation and digestion. *Journal of Agricultural and Food Chemistry, 66*, 1461–1471.

Zou, Y., Guo, J., Yin, S. W., Wang, J. M., & Yang, X. Q. (2015). Pickering emulsion gels prepared by hydrogen-bonded zein/tannic acid complex colloidal particles. *Journal of Agricultural and Food Chemistry, 63*, 7405–7414.